

## ORIGINAL ARTICLE

# Novel needle-type electrocoagulation and combination pharmacotherapy: Basic and clinical studies on efficacy and safety in treating keloids

Jingting Zhao MM<sup>1</sup> | Xiaoyu Zhai MM<sup>1,2</sup> | Zhiyi Xu MM<sup>1,2</sup> | Shu Zhou MM<sup>1</sup> |  
Liqun Gu MM<sup>1</sup> | Lin Chen MM<sup>3</sup> | Bingrong Zhou MD<sup>4</sup> | Hui Hua MD<sup>1</sup>

<sup>1</sup>Department of Dermatology, Nantong Third People's Hospital, Affiliated Nantong Hospital 3 of Nantong University, Nantong, China

<sup>2</sup>Medical School of Nantong University, Nantong, China

<sup>3</sup>Nantong Institute of Liver Diseases, Nantong Third People's Hospital, Affiliated Nantong Hospital 3 of Nantong University, Nantong, China

<sup>4</sup>Department of Dermatology, The First Affiliated Hospital of Nanjing Medical University, Nanjing, China

## Correspondence

Hui Hua, Department of Dermatology, Nantong Third People's Hospital, Affiliated Nantong Hospital 3 of Nantong University, Nantong 226001, China.  
Email: [huahui@ntu.edu.cn](mailto:huahui@ntu.edu.cn)

Bingrong Zhou, Department of Dermatology, The First Affiliated Hospital of Nanjing Medical University, Nanjing 210029, China.  
Email: [zhoubingrong@njmu.edu.cn](mailto:zhoubingrong@njmu.edu.cn)

## Funding information

Natural Science Foundation of Nantong Municipality, Grant/Award Number: MS22022102

## Abstract

**Background and Aim:** Keloids cannot be effectively treated using monotherapy regimens. This study aimed to evaluate the efficacy and safety of ablation (a novel needle-assisted electrocoagulation technique) combined with pharmacotherapy (corticosteroid and 5-fluorouracil [5-FU] injections) in removing keloids and to investigate the underlying biological mechanisms.

**Methods:** The effects of energy consumption and duration of needle-assisted electrocoagulation on the ablation zone were tested in porcine liver tissue, which simulates human skin. The regulatory effects of ablation combined with pharmacotherapy on collagen deposition, cell proliferation, and angiogenesis were analyzed in a keloid-bearing nude mouse model in vivo. In a clinical trial involving six patients with keloids, the Vancouver Scar Scale (VSS) and Patient and Observer Scar Assessment Scale (POSAS) scores were graded before treatment and 1 month after one cycle of ablation combined with corticosteroid and 5-FU therapy.

**Results:** Higher energy consumption and longer duration of electrocoagulation resulted in a larger ablation zone and higher surface temperature. Ablation combined with pharmacotherapy significantly reduced keloid volume in nude mice, upregulated MMP-1 and MMP-3, downregulated COL I and COL III, and inhibited angiogenesis and proliferation. This combination also significantly reduced the VSS and POSAS scores in patients with keloids after treatment without any obvious adverse events.

**Conclusion:** Our findings show that electroablation combined with pharmacotherapy effectively reduces keloid volume by inhibiting collagen deposition, angiogenesis, and cell proliferation. Thus, this novel combination may serve as a safe therapeutic approach for keloid removal.

## KEYWORDS

collagen, electrolysis, keloid, laser ablation

Jingting Zhao, Xiaoyu Zhai, and Zhiyi Xu contributed equally.

This is an open access article under the terms of the [Creative Commons Attribution](https://creativecommons.org/licenses/by/4.0/) License, which permits use, distribution and reproduction in any medium, provided the original work is properly cited.

© 2024 The Author(s). *Journal of Cosmetic Dermatology* published by Wiley Periodicals LLC.

## 1 | INTRODUCTION

Keloids are a fibroproliferative disorder characterized by the excessive growth of extra scar tissue. They invade normal or healthy skin, leading to clinical symptoms of itching, pain, pulling sensation, or local functional impairment that significantly affect quality of life.<sup>1</sup> Epidemiological data have revealed that the global prevalence of keloids ranges from 1% to 16%, being higher among non-Caucasians than Caucasians.<sup>2</sup> The pathological mechanisms of keloids are complicated and mainly involve abnormal wound healing, excessive fibroblast proliferation, abnormal collagen accumulation, and sustained inflammatory responses.<sup>3</sup> Excessive collagen deposition is essential for the formation of keloids and their characteristic appearance.

Optional therapeutic strategies for keloids include intralesional injections, laser therapy, surgical removal, and superficial radiotherapy.<sup>4</sup> Intralesional injection of corticosteroids, the first-line therapy for keloids, promotes collagenase production and mediates fibroblast proliferation and collagen synthesis.<sup>5</sup> However, corticosteroid monotherapy is limited by its low efficacy and high incidence of adverse events, such as skin atrophy, capillary dilation, and pigment reduction. Fractional CO<sub>2</sub> lasers are efficient for the treatment of keloids; however, they cause thermal damage, epidermal loss, and adverse events such as pain, edematous erythema, and scab formation. A combination of corticosteroids and 5-fluorouracil (5-FU) is superior to monotherapy in removing keloids with a lower recurrence rate.<sup>6</sup> Similarly, fractional CO<sub>2</sub> laser combined with pharmacotherapy achieves higher efficacy and lower recurrence rates than single intralesional injection of corticosteroids.<sup>7</sup> Therefore, combination treatment is a promising alternative for patients with keloids.

Thermal ablation has emerged as a method to achieve coagulative necrosis and vascular occlusion by converting the energy generated by electrical currents into heat.<sup>8</sup> Accumulating evidence has shown the effectiveness of thermal ablation for various types of cancers.<sup>9,10</sup> Electrocoagulation is a thermal ablation technique usually used as an adjunctive treatment in surgical procedures. It produces a lower temperature (below 100°C) than that produced by CO<sub>2</sub> laser, which heats tissues to 300°C. The mild heat generated by electrocoagulation induces cellular dehydration, protein denaturation, tissue devitalization, and closure of small blood vessels without causing excessive thermal damage. Wu et al.<sup>11</sup> confirmed the efficacy and safety of electrocoagulation in the successful treatment of six cases of unresectable ampullary tumors. However, whether electrocoagulation has a similar therapeutic effect on keloids remains unclear.

In this study, electrocoagulation for thermal ablation was performed using a needle-assisted electrode to deliver energy directly into the dermis, followed by pharmacotherapy with corticosteroid and 5-FU injections. The safety of this combination treatment was analyzed based on surface temperature and duration of thermal ablation in a simulated *in vitro* model, and its effectiveness on keloids was validated in an *in vivo* mouse model and a clinical trial.

## 2 | METHODS

### 2.1 | Needle-assisted electrocoagulation for thermal ablation

Electrocoagulation was performed using a high-frequency electro-surgical unit with an ablation injection needle (Healthsea, China) 32.5 mm in length and 0.6 mm in width. The negative electrode plate was attached to the experimental tissue, with a yellow indicator light confirming good contact. The time controller was connected to the footswitch interface of the high-frequency electrosurgical unit to set the duration of energy release (Figure 1).

### 2.2 | Measurement of electrothermal ablation area in porcine liver tissue

Fresh porcine liver tissue was obtained and stored at 36 ± 1°C. A tip spacing greater than 3 cm was applied to minimize the impact of electrocoagulation on the surrounding tissues. A needle-assisted energy delivery device, 1 cm in length, was vertically inserted into the porcine liver for electrocoagulation, and the width of the ablation zone was measured. The electrocoagulation power was set to 20–80 W for 0.5, 1, and 2 s.

### 2.3 | Measurement of surface temperature of porcine liver tissue during electrothermal ablation

A noncontact infrared thermometer (HIKVISION H13) with 19 200 pixels (160 × 120) and a temperature range of –20 to 350°C was used to thermally visualize liver tissue ablated by electrocoagulation. A needle-assisted energy delivery device was inserted into the liver tissue at a 30° angle for electrocoagulation, and the surface temperature was measured 15 cm from the liver tissue. The electrocoagulation power was set to 20–80 W for 0.5, 1, and 2 s.

### 2.4 | Construction of a keloid-bearing nude mouse model

Human keloid specimens were obtained surgically, in accordance with the ethical principles of the Declaration of Helsinki. The research protocol was approved by the Ethics Committee of the Third People's Hospital of Nantong (EL2022016). The keloid specimens were devoid of epidermal and adipose tissues and were cut into tissue blocks measuring 6 mm × 6 mm × 4 mm.

The study strictly adhered to the protocols sanctioned by the Animal Center at the Medical College of Nantong University (S20230426-009). Briefly, male BALB/c-nu nude mice (4–6 weeks of age and weighing 18 ± 2 g) were raised in a specific pathogen-free (SPF) environment. All animals underwent a 2-week acclimation period until they weighed 20 ± 2 g before transplantation. A 6-mm

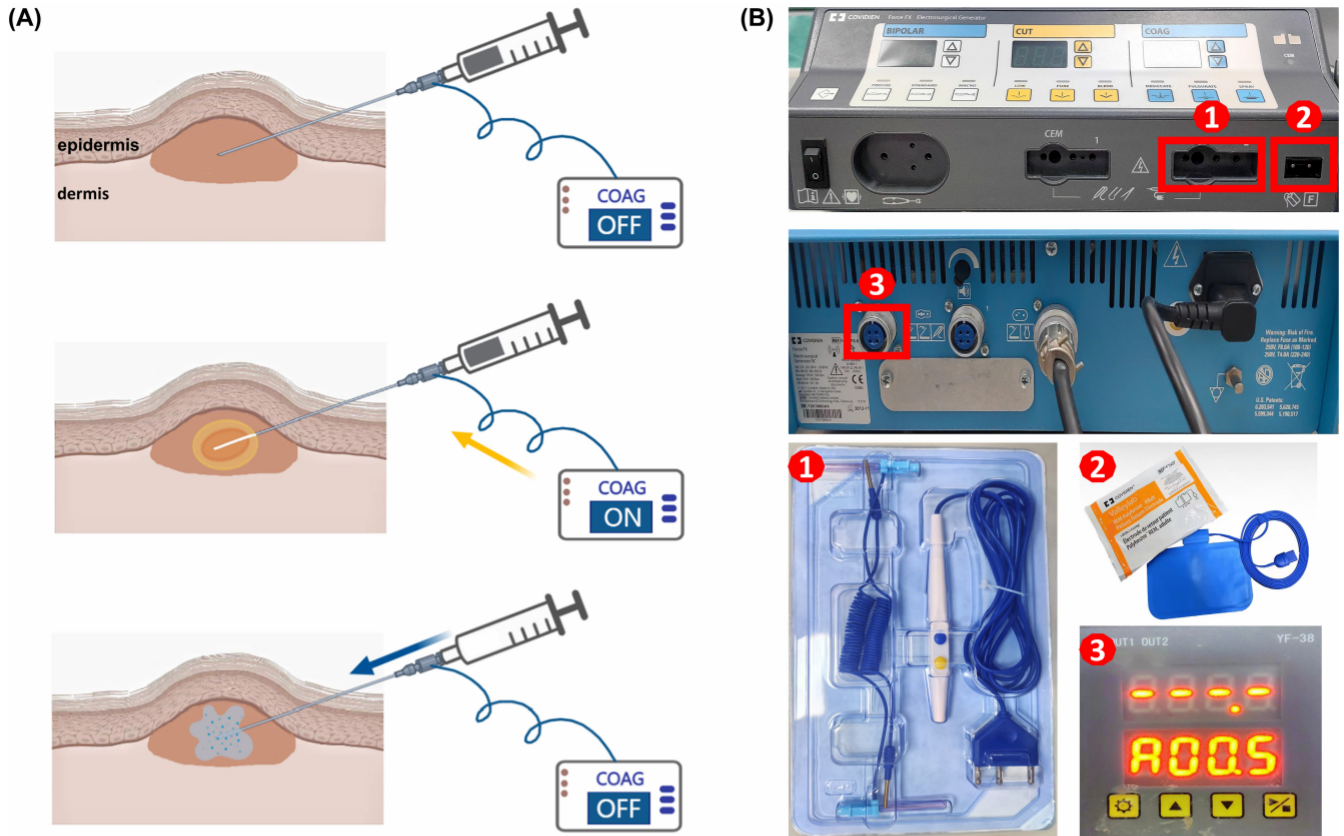


**FIGURE 1** Schematic diagram of the treatment process and equipment for ablation combined with pharmacotherapy. (A) Keloid tissue was first managed by thermal ablation using needle-assisted electrocoagulation, followed by intraleisional injections of a corticosteroid and 5-FU. (B) The needle-assisted electrocoagulation device (1. electrocoagulation device and its connection with the serial number; 2. the negative plate and its connection with the serial number; 3. the time control device and its connection).

incision was made on both sides of the shoulder blades using ophthalmic scissors to allow subcutaneous implantation of the keloid tissue blocks. After implanting the keloid tissue, the nude mice were housed in separate cages.

## 2.5 | Ablation combined with pharmacotherapy in treating keloids in mice

One week after the implantation of keloid tissue, the mice were randomly divided into the CONTROL (blank control), COAG (50W power electrocoagulation for 0.5s), GC+5-FU (local injection of a 5:1 mixture containing 1 mg/mL betamethasone and 25 mg/mL fluorouracil at a total volume of 0.1 mL), and COAG+GC+5-FU (drug injection as mentioned above immediately after electrocoagulation) groups, with five mice per group. Subcutaneous keloid tissues were removed, weighed, and photographed 7 days after treatment. Throughout the experiment, the parameters of the keloid xenografts in the nude mice, specifically their length, width, and height, were assessed every 3 days using a precision caliper. These measurements were subsequently used to determine the tissue volume for further analysis.

## 2.6 | Hematoxylin and eosin, Masson's trichrome, and immunohistochemistry staining

Keloid tissues were fixed with 4% paraformaldehyde, embedded in paraffin, and cut into sections of 3–5  $\mu$ m thickness. After deparaffinization, the sections were immersed in antigen retrieval solution (20 $\times$ Tris-EDTA, pH 9.0), 3% hydrogen peroxide solution, and blocking agent (3% BSA) and then incubated with rabbit anti-CD31, rabbit anti-PCNA, rabbit anti-MMP1, rabbit anti-MMP3, rabbit anti-collagen I, and rabbit anti-collagen III antibodies, followed by horseradish peroxidase-labeled secondary antibodies (Servicebio, Wuhan, China). Hematoxylin and eosin (H&E) and Masson's trichrome staining were used for visualization under a microscope.

## 2.7 | Quantitative reverse transcription polymerase chain reaction (qRT-PCR)

Total cellular RNA was extracted using TRIzol reagent (Takara, Shiga, Japan), and 1000 ng of the extracted RNA was reverse-transcribed into cDNA using the PrimeScript RT kit (Takara, Shiga, Japan). The qRT-PCR was performed on a Bio-Rad CFX system (Bio-Rad,



Munich, Germany) using TB Green Premix Ex Taq II (Takara, Shiga, Japan). The relative expression of the target genes was normalized to that of ACTB using the  $2^{-\Delta\Delta C_t}$  method. Primer sequences (Sangon Biotech, Shanghai, China) and shRNAs used for qRT-PCR are provided in Supplementary Materials.

## 2.8 | Human subjects

Six patients, including three males and three females, who visited the Outpatient Department of the Third People's Hospital of Nantong City were selected. The research protocol was approved by the Ethics Review Committee of the Third People's Hospital of Nantong City Affiliated with Nantong University (EL2022016). The inclusion criteria were as follows:  $\geq 18$  years of age, normal physical and mental health, willing to complete the treatment course and attend follow-up visits, and provision of written informed consent. We excluded pregnant or lactating women, individuals with skin tumors, systemic diseases, immunosuppression, scar lesions combined with infection or bleeding, individuals currently using oral anticoagulants, and those who had been managed with other keloid treatments within the past 6 months. The causes and anatomical sites of keloids of the included participants are detailed in Table 3.

## 2.9 | Clinical trial planning

Eligible subjects with keloids who enrolled for the clinical trial were managed by routine skin disinfection, local infiltration anesthesia around the keloid using lidocaine, electrocoagulation with the needle electrode inserted into the keloid (energy release according to tissue thickness), and local injection of a 5:1 mixture of 1 mg/mL betamethasone and 25 mg/mL fluorouracil in the total volume based on tissue size. The treatment was performed for three sessions over 3 weeks, with the released energy adjusted based on the thickness of the keloid. An ice pack was applied to the ablation site to avoid excessive heat stimulation or damage to the epidermal layer. The patients were advised to avoid friction, scratching, and sunlight exposure after treatment.

## 2.10 | Scar assessment of keloids

Standardized digital photos of keloids were captured before and 1 month after treatment and assessed using the Vancouver Scar Scale (VSS) and Patient and Observer Scar Assessment Scale (POSAS) scores. The VSS was used to determine changes in the color, pliability, thickness, and vascularity of the keloids. The POSAS consists of two subscales for patients (Patient Scar Assessment Scale; PSAS) and observers (Observer Scar Assessment Scale; OSAS). The PSAS was used to measure itching, pain, color, hardness, thickness, and overall appearance, whereas the OSAS was used to measure vascularity, color, thickness, roughness, pliability, and keloid surface area. The VSS and OSAS items were scored by two dermatologists to calculate the mean scores.

## 2.11 | Statistical analysis

Statistical analysis was conducted using SPSS 26.0 software (Version 26.0. Armonk, NY: IBM Corp.). The normality of the data distribution was assessed using the Kolmogorov-Smirnov test. Data with a normal distribution are expressed as mean  $\pm$  standard deviation (SD), and differences between groups were analyzed using the paired sample *t*-test. Data that were not normally distributed are expressed as medians (minimum and maximum), and differences between groups were analyzed using the paired sample Wilcoxon signed-rank test. Statistical significance was set at  $p < 0.05$ .

## 3 | RESULTS

### 3.1 | Optimal parameters of electrocoagulation for keloid treatment

The parameters of electrocoagulation between 20 and 60 W for 0.5 s, 20 and 50 W for 1 s, and 20 and 40 W for 2 s were confirmed to be safe (provide a surface temperature lower than 60°C<sup>13</sup>) without causing obvious wounds on the surface of the porcine liver tissues (Figure 2A, Table 1). The widest ablation area was observed around the needle tip (Figure 2B, Table 2). Electrocoagulation at 30, 40, 50, and 60 W for 0.5 s successfully ablated tissues at widths of  $1.16 \pm 0.32$ ,  $1.45 \pm 0.29$ ,  $1.81 \pm 0.24$ , and  $2.23 \pm 0.25$  mm, respectively. Within the same range of ablation power, electrocoagulation for 1 s successfully ablated tissues at widths of  $0.86 \pm 0.07$ ,  $1.65 \pm 0.11$ ,  $2.32 \pm 0.1$ , and  $3.15 \pm 0.26$  mm, respectively; and  $1.87 \pm 0.12$ ,  $2.85 \pm 0.21$ ,  $3.55 \pm 0.33$ , and  $4.6 \pm 0.22$  mm for 2 s, respectively. A higher power and longer duration of electrocoagulation resulted in a larger area of ablation.

### 3.2 | Ablation combined with pharmacotherapy inhibits the growth of keloids in vivo

Compared to mice in the CONTROL group, tissue volume was significantly decreased in animals treated with electrocoagulation, drug injection, or both (Figure 3A). The most pronounced reduction in keloids was observed in the COAG+GC+5-FU group, with a decrease in volume by  $39.67 \pm 1.44\%$  compared to the CONTROL group (Figure 3A,  $p < 0.001$ ).

### 3.3 | Ablation combined with pharmacotherapy inhibits angiogenesis and cell proliferation of keloids in vivo

H&E staining revealed a larger number of fibroblasts and excessive accumulation and disorderly arrangement of collagen fibers in keloid tissues of animals in the CONTROL group (Figure 4A). Electrocoagulation or drug injection significantly decreased the



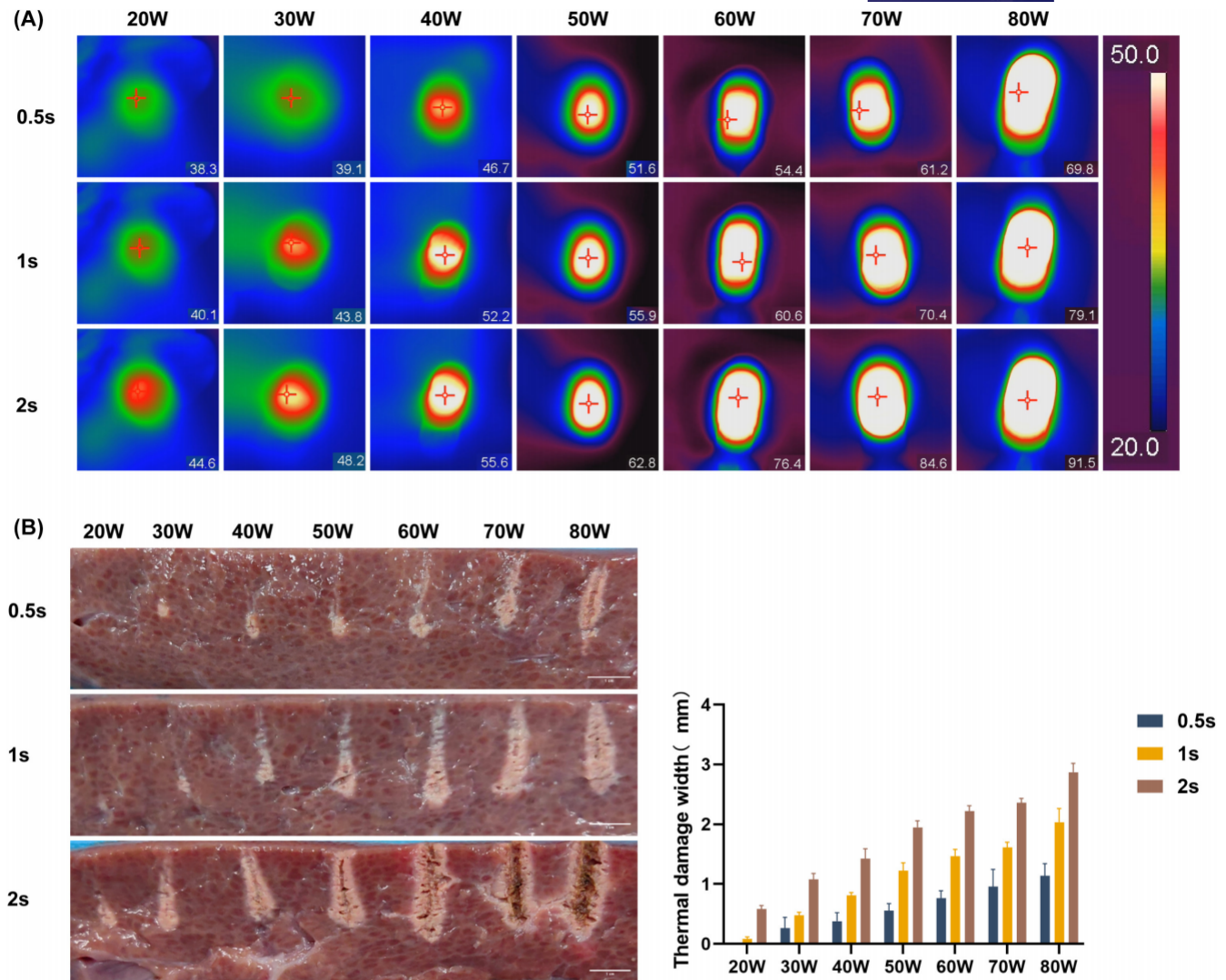


**FIGURE 2** Optimal parameters for needle-assisted electrocoagulation in keloid treatment. (A) Surface temperature of porcine liver tissue after electrocoagulation with varying energies and durations. (B) Representative visualizations of the thermal ablation zone after electrocoagulation treatment at 20–80W for 0.5–2s (left) and quantitative analysis of the width of ablation zone (right). Scale bar=1 cm.

**TABLE 1** Surface temperature of porcine liver tissue after electrocoagulation at varying energies and times.

	0.5s (°C)	1.0s (°C)	2.0s (°C)
20W	38.37±0.31	41.5±1.4	45.63±1.23
30W	38.9±1.41	43.7±0.66	49.77±1.6
40W	47.23±2.25	52.03±2.06	56.73±1.47
50W	49.57±2.41	58.1±5.07	64.9±3.13
60W	56.2±2.16	63.83±2.82	73.3±2.82
70W	61.53±0.42	70.63±4.75	83.33±1.1
80W	67.37±2.5	78.7±4.31	88.3±5.37

**TABLE 2** Width of the ablation zone in porcine liver tissues after electrocoagulation at varying energies and times.

	0.5s (mm)	1.0s (mm)	2.0s (mm)
20W		0.86±0.07	1.87±0.12
30W	1.16±0.32	1.65±0.11	2.85±0.21
40W	1.45±0.29	2.32±0.10	3.55±0.33
50W	1.81±0.24	3.15±0.26	4.6±0.22
60W	2.23±0.25	3.63±0.23	5.14±0.18
70W	2.62±0.57	3.92±0.18	5.42±0.15
80W	2.97±0.42	4.77±0.45	6.44±0.30

number of fibroblasts and alleviated the excessive accumulation and irregular arrangement of collagen fibers in the dermal layer; this effect was more pronounced in the COAG+GC+5-FU group. Notably, the histological changes were more severe at the center of the ablated tissue. We further examined the expression of CD31 and PCNA in keloid tissues by immunohistochemistry (IHC) staining

to evaluate angiogenesis and proliferation, respectively. The expression of CD31 in the COAG and GC+5-FU groups was significantly lower than that in the CONTROL group (Figure 4B). The microvessel density in the COAG+GC+5-FU group showed the most significant decrease, from  $34.33 \pm 4.16$  to  $13 \pm 1.73$  ( $p < 0.01$ ). PCNA was significantly expressed in keloid tissues in the CONTROL

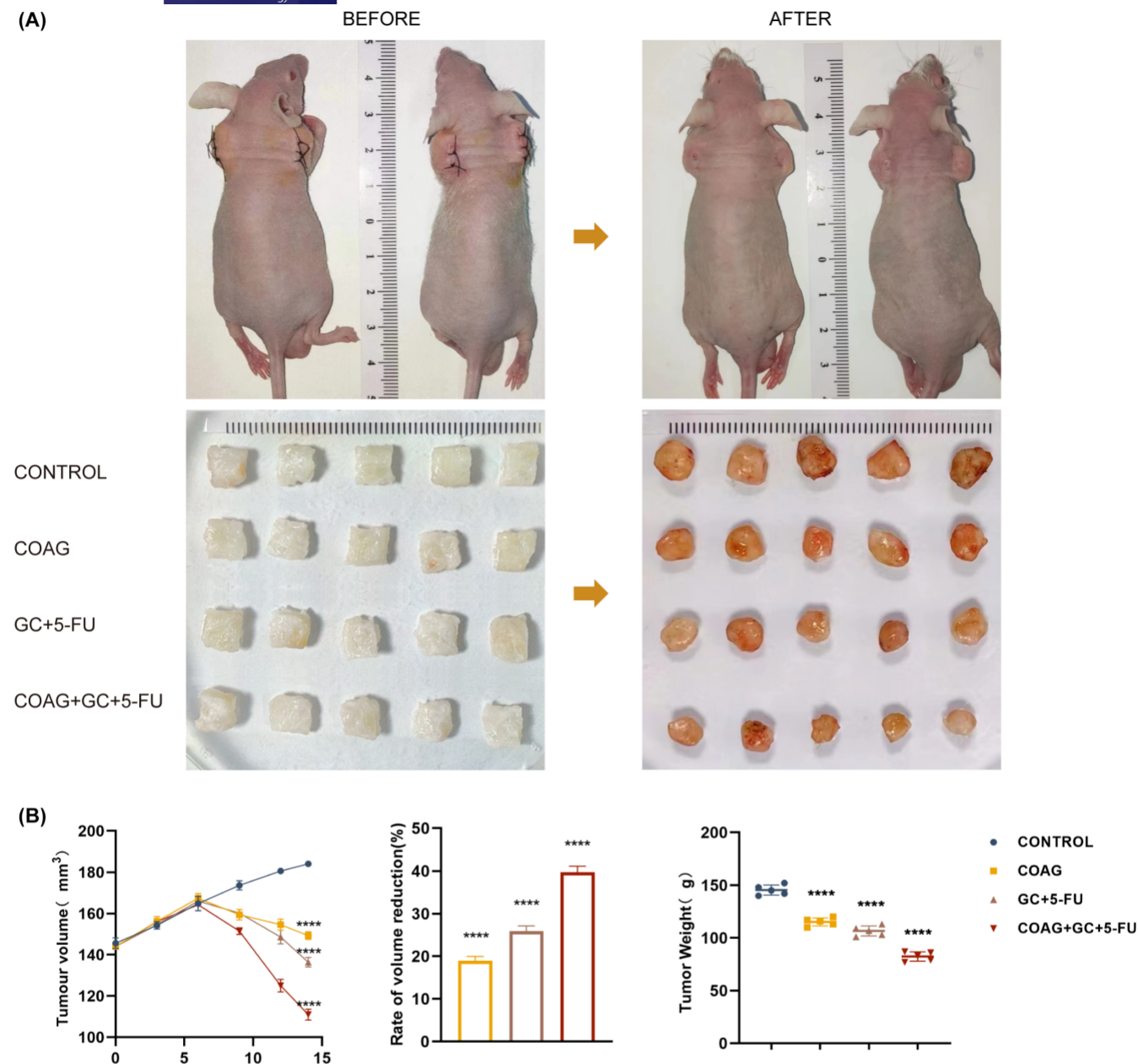


**FIGURE 3** Ablation combined with pharmacotherapy inhibits the growth of keloids in vivo. (A) Representative images of nude mice that were subcutaneously implanted keloid tissues before and after treatment (upper lane). Implanted keloid tissues after treatment were collected (bottom lane). (B) Changes in the weight, volume, and volume inhibition rate of keloids in nude mice.  $n = 5$ . \*\*\*\* $p < 0.0001$ .

group compared to the other groups. The proportion of PCNA-positive cells was mostly reduced in COAG + GC + 5-FU group from  $74.34\% \pm 5.23\%$  to  $33.57\% \pm 4.86\%$  (Figure 4C;  $p < 0.01$ ).

### 3.4 | Ablation combined with pharmacotherapy upregulates metalloproteinases and downregulates collagens

Histological changes in the thickened and disordered collagen fibers in keloid tissues were significantly alleviated by electrocoagulation or drug treatment, especially in the COGA + GC + 5-FU group (Figure 5A). Metalloproteinases (MMPs) possess the ability to degrade and metabolize the extracellular matrix. IHC staining showed

that the expression levels of MMP-1 and MMP-3 were significantly elevated, whereas those of Col I and Col III were reduced, following electrocoagulation or drug treatment (Figure 5B,C;  $p < 0.05$ ). Similar changes were detected at the mRNA level (Figure 5D), with the most significant changes in the expression levels of MMPs and collagens being detected in the COAG + GC + 5-FU group ( $p < 0.01$ ).

### 3.5 | Ablation combined with pharmacotherapy alleviates clinical signs and symptoms in patients with keloids

We conducted a clinical trial involving six eligible patients with keloids. There were three males and three females with a mean age



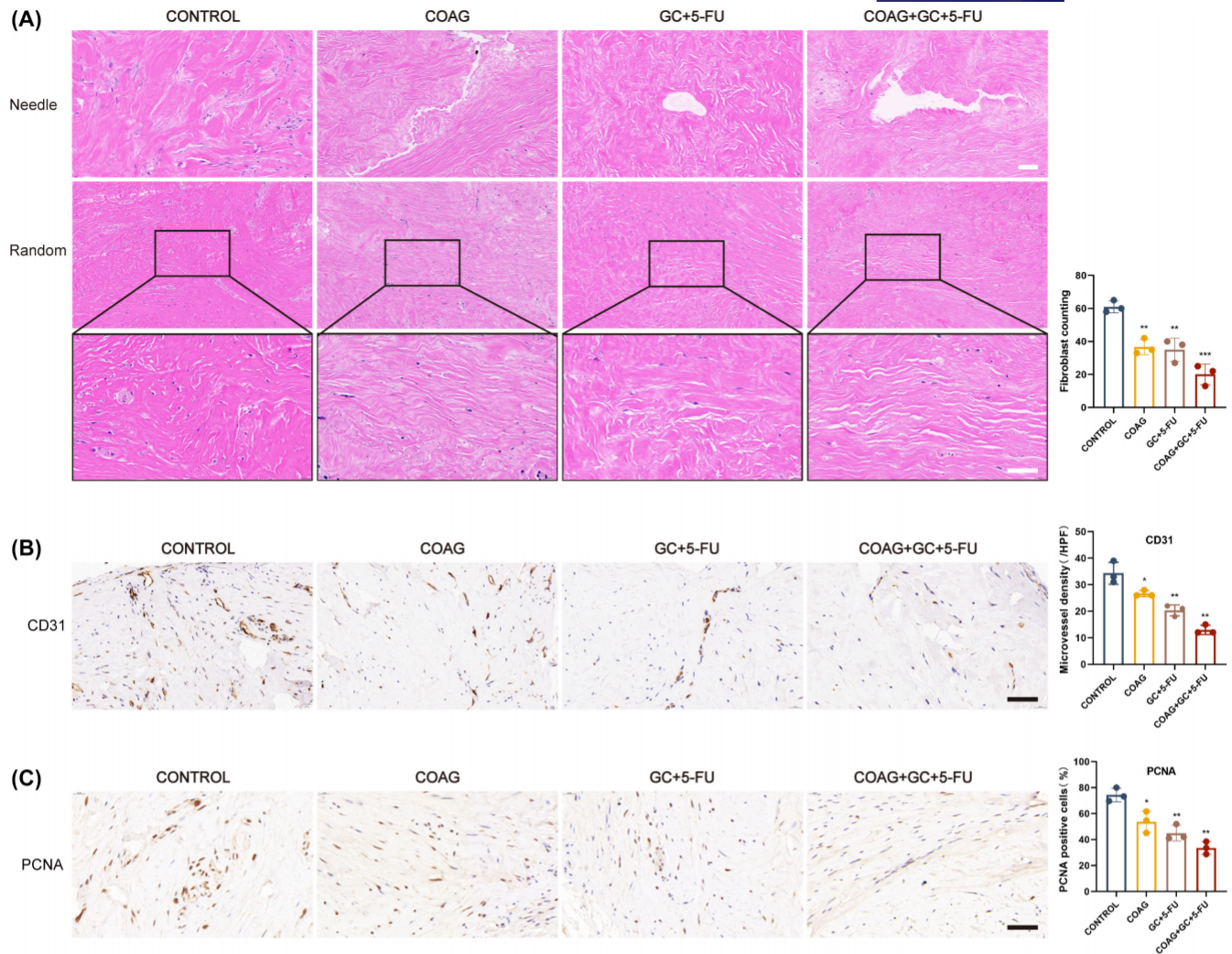


**FIGURE 4** Ablation combined with pharmacotherapy inhibits angiogenesis and cell proliferation of keloids in vivo. (A) H&E staining of keloids from nude mice and the number of fibroblasts. Scale bar = 50  $\mu$ m. (B) Immunohistochemistry (IHC) staining of CD31 and microvessel density in keloids from nude mice. Scale bar = 50  $\mu$ m. (C) IHC staining of PCNA and percentage of positive cells in keloids from nude mice. Scale bar = 50  $\mu$ m.  $n=5$ . \* $p<0.05$ , \*\* $p<0.01$ , \*\*\* $p<0.001$ .

of 26.5 years and a disease duration of 4.7 years. Most keloids were located on the head and neck, and the main causes were acne, folliculitis, and trauma (Table 3). After 28 days of treatment, the total VSS score and the scores for pigmentation, vascularity, height, and pliability were significantly lower than those at baseline ( $p<0.05$ ; Table 4). The total scores on both OSAS and PSAS subscales were significantly reduced after 28 days of treatment (Tables 5 and 6). In the OSAS group, the posttreatment scores for thickness, roughness, and softness were significantly reduced ( $p<0.05$ ), while those for vascular distribution, color, and surface area were comparable to those at baseline ( $p>0.05$ ). The scores for all items in the PSAS, except color, significantly decreased after treatment ( $p<0.01$ ). Therefore, we considered this clinical trial a preliminary validation of the efficacy of ablation combined with pharmacotherapy in patients with keloids (Figure 6).

## 4 | DISCUSSION

The present study demonstrated the efficacy of ablation combined with pharmacotherapy for treating keloids both in mice and humans. First, we analyzed the optimal parameters for needle-assisted electrocoagulation in porcine liver tissues to ensure therapeutic efficacy and maintain epidermal integrity. In a keloid-bearing nude mouse model, electrocoagulation combined with local drug injection of a corticosteroid and 5-FU significantly reduced the volume of keloids; inhibited angiogenesis, proliferation, and deposition of the extracellular matrix; and promoted collagen degradation. A clinical trial involving six patients further validated the efficacy of ablation combined with pharmacotherapy for keloid removal.

Porcine liver is usually used to simulate human skin tissue and was applied here to determine the safety of energy release and duration



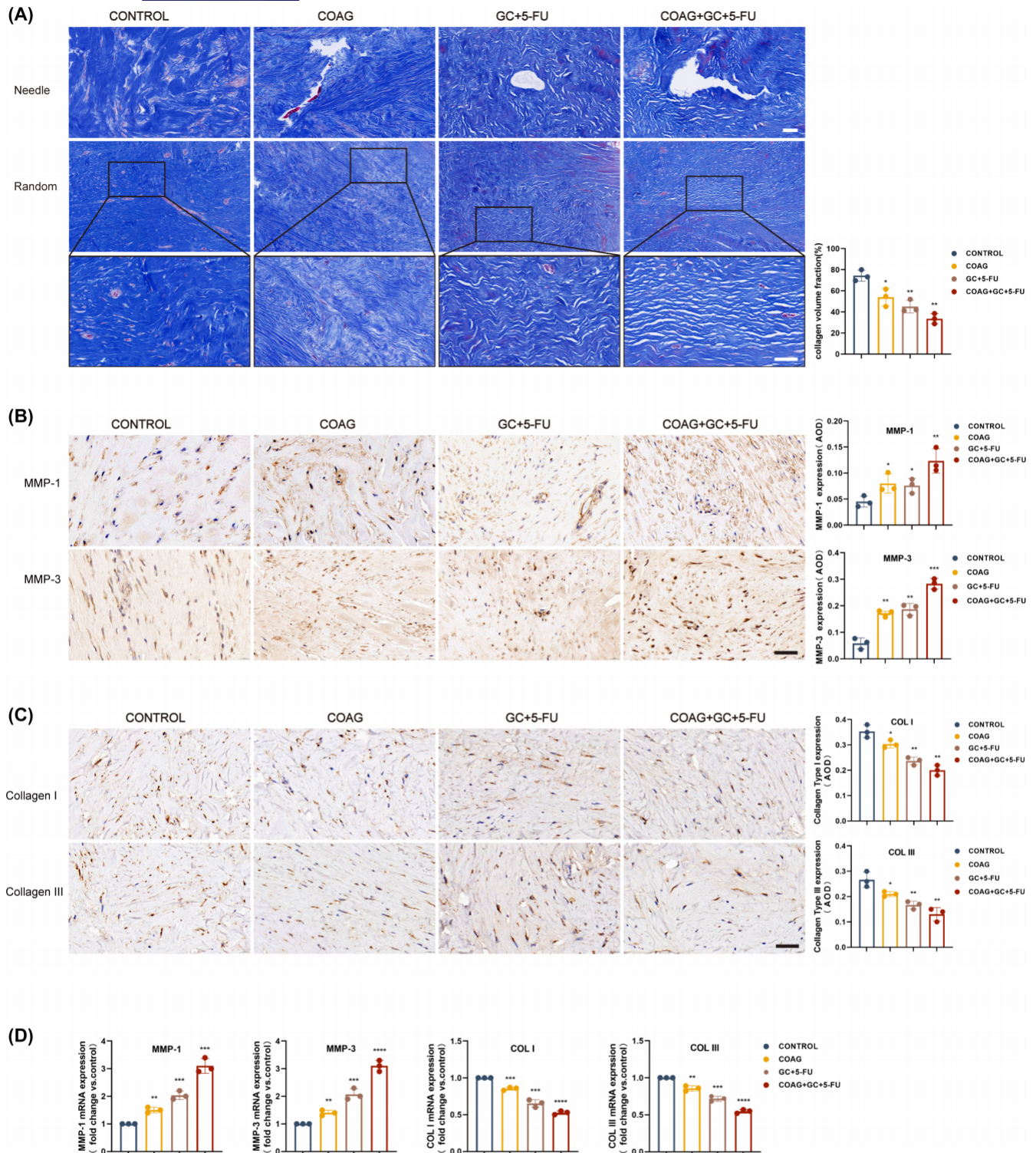


**FIGURE 5** Ablation combined with pharmacotherapy upregulates MMPs and downregulates collagens. (A) Masson's trichrome staining and quantitative analysis of keloids from nude mice. Scale bar = 50  $\mu$ m. (B) Immunohistochemistry (IHC) staining of MMP-1 and MMP-3 in keloids from nude mice. Scale bar = 50  $\mu$ m. (C) IHC staining of COL I and COL III in keloids from nude mice. Scale bar = 50  $\mu$ m. (D) The mRNA levels of MMP-1, MMP-3, COL I, and COL III in keloids from nude mice. Scale bar = 50  $\mu$ m.  $n = 5$ . \* $p < 0.05$ , \*\* $p < 0.01$ , \*\*\* $p < 0.001$ , \*\*\*\* $p < 0.0001$ .

of electrocoagulation.<sup>13</sup> In this study, we used ex vivo pig liver tissue as a surrogate model for keloids to assess and determine suitable parameters. We observed that the ablation zone in the porcine liver tissue was centered at the tip of the electrode, and with increasing

energy, it gradually expanded along to the entire periphery of the energy delivery device, which is consistent with the results of Taheri et al.<sup>14</sup> Hantash et al.<sup>15</sup> suggested that the damage to the epidermis could be effectively prevented by achieving the maximum heating

**TABLE 3** Clinical characteristics of patients with keloids ( $n = 6$ ).

Case	Sex	Age (years)	Duration (years)	Location	Cause
1	Female	32	5	Right subaxillary	Trauma
2	Male	25	3	Left shoulder	Folliculitis
3	Female	35	8	Right subaxillary	Trauma
4	Male	28	5	Right mandible	Acne
5	Male	21	3	Right mandible	Acne
6	Female	18	4	Right mandible	Acne

**TABLE 4** VSS scores in patients with keloids before and after ablation combined with pharmacotherapy ( $n = 6$ ).

	VSS score		Z/T	p Value
	Before treatment	After treatment		
Pigmentation	3.00 (1.75, 3.00)	2.00 (1.75, 2.00)	-1.414	0.157
Vascularity	2.34 $\pm$ 0.82	1.34 $\pm$ 1.03	1.936	0.111
Height	3.00 (2.50, 3.25)	1.00 (0.00, 1.25)	-2.232	0.026
Pliability	3.00 (2.75, 3.00)	0.00 (0.00, 1.00)	-2.251	0.024
Total score	10.50 $\pm$ 1.76	4.34 $\pm$ 1.86	4.936	0.004

Note: Normally distributed data are expressed as mean  $\pm$  SD and were compared using the paired sample t-test; otherwise, data are expressed as median (minimum, maximum) and were compared using the paired sample Wilcoxon signed-rank test.

Abbreviation: VSS, Vancouver Scar Scale.

**TABLE 5** PSAS scores in patients with keloids before and after ablation combined with pharmacotherapy ( $n = 6$ ).

	PSAS score		Z/T	p Value
	Before treatment	After treatment		
Vascularity	5.17 $\pm$ 1.51	3.00 $\pm$ 2.30	2.270	0.072
Pigmentation	5.00 $\pm$ 1.22	3.33 $\pm$ 2.11	1.569	0.177
Thickness	4.33 $\pm$ 1.29	0.67 $\pm$ 0.60	5.966	0.002
Relief	4.25 $\pm$ 1.91	2.25 $\pm$ 2.23	3.464	0.018
Pliability	5.00 (3.88, 5.13)	0.25 (0.00, 2.25)	-2.201	0.028
Surface area	4.50 $\pm$ 1.52	2.75 $\pm$ 2.23	2.406	0.061
Total score	27.92 $\pm$ 6.42	12.75 $\pm$ 7.76	4.602	0.006

Note: Normally distributed data are expressed as mean  $\pm$  SD and were compared using the paired sample t-test; otherwise, data are expressed as median (minimum, maximum) and were compared using the paired sample Wilcoxon signed-rank test.

Abbreviation: PSAS, Patient Scar Assessment Scale.

**TABLE 6** OSAS scores in patients with keloids before and after ablation combined with pharmacotherapy ( $n = 6$ ).

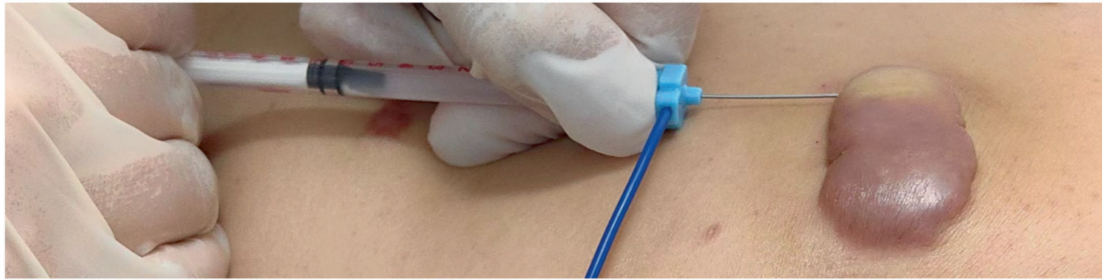
	OSAS score		Z/T	p Value
	Before treatment	After treatment		
Pain	3.00 $\pm$ 2.10	1.50 $\pm$ 1.64	3.503	0.017
Pruritus	4.00 $\pm$ 2.53	1.83 $\pm$ 1.47	3.993	0.01
Color difference	3.50 (3.00, 6.25)	4.00 (1.75, 4.00)	-1.633	0.102
Stiffness	5.67 $\pm$ 1.75	1.50 $\pm$ 1.05	4.382	0.007
Thickness	6.66 $\pm$ 0.73	1.67 $\pm$ 1.37	4.108	0.009
Irregularity	6.00 $\pm$ 2.37	3.67 $\pm$ 1.37	3.796	0.013
Total score	3.00 $\pm$ 2.10	1.50 $\pm$ 1.64	3.503	0.017

Note: Normally distributed data are expressed as mean  $\pm$  SD and were compared using the paired sample t-test; otherwise, data are expressed as median (minimum, maximum) and were compared using the paired sample Wilcoxon signed-rank test.

Abbreviation: OSAS, Observer Scar Assessment Scale.



(A)



(B)



(C)

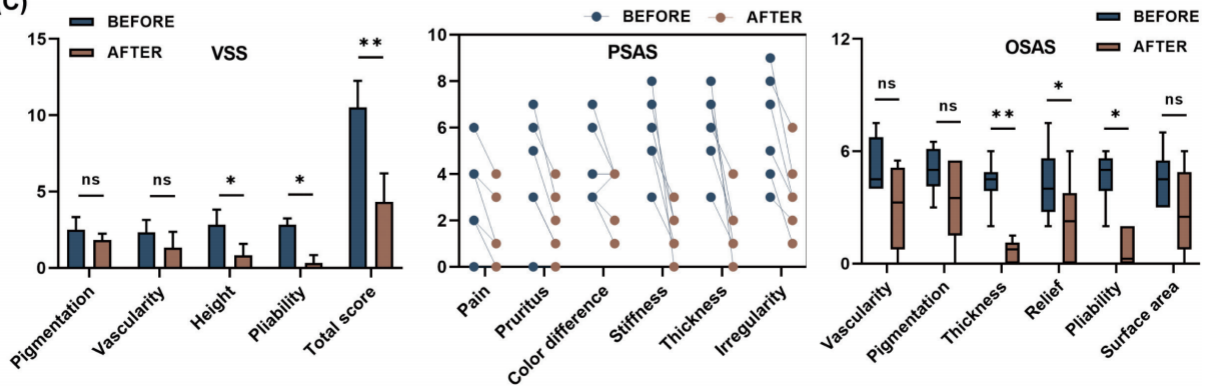




**FIGURE 6** Ablation combined with pharmacotherapy alleviates clinical signs and symptoms in patients with keloids. (A) Representative image of ablation combined with pharmacotherapy in human keloid treatment. (B) Keloids before (top image) and after (bottom image) ablation combined with pharmacotherapy. (C) The VSS and POSAS scores of patients with keloids before and after ablation combined with pharmacotherapy.  $n=6$ . \* $p<0.05$ , \*\* $p<0.01$ ; ns, no significant difference.

effect around the tip of the electrode in the dermis. Needle-assisted electrocoagulation generates a higher temperature in the dermal layer to melt collagen but a lower temperature in the epidermis. Our study revealed that by applying electrocoagulation energy in the ranges of 20–60W for 0.5s, 20–50W for 1s, and 20–40W for 2s, the temperature on the epidermis could be kept below 60°C. This facilitates the preservation of epidermal integrity, thereby safeguarding epidermal cells from irreversible harm and undesirable outcomes such as infection and pigmentation.<sup>15</sup>

Deposition of the extracellular matrix plays a pivotal role in various fibrotic diseases. In the keloid-bearing nude mouse model, we observed that needle-assisted electrocoagulation significantly up-regulated MMP-1 and MMP-3 and downregulated COL I and COL III in keloid tissues. Additionally, we observed that electrocoagulation degraded collagen and occluded blood vessels through thermal ablation. Craig et al.<sup>16</sup> reported that MMPs are the primary anti-fibrotic warriors responsible for breaking down and metabolizing the extracellular matrix. They prevent scar formation and angiogenesis by downregulating cytokines associated with cell proliferation and migration in fibroblasts.<sup>17,18</sup> Herein, electrical stimulation promoted the expression of MMPs, even in the absence of thermal stimulation, leading to the suppression of fibrosis in keloids. Therefore, we believe that needle-assisted electrocoagulation, beyond its role in occluding blood vessels and reshaping denatured collagen through thermal ablation,<sup>19</sup> could also elicit collagen degradation and inhibit proliferation and angiogenesis by promoting the expression of MMPs through electrical stimulation.

Ablation combined with pharmacotherapy was also effective in patients with keloids. After three treatments, the patients' VAA and POSAS scores significantly improved. Our therapeutic strategy was superior to other treatments involving open wounds as it streamlined postoperative care and abbreviated the recovery period. The duration of epidermal wound healing correlates with scar formation, and delayed healing may contribute to a higher degree of fibrosis.<sup>20</sup> Preserving the integrity of the epidermis is important in lowering the recurrence rate of keloids and the incidence of adverse events, such as swelling, erythema, and infection.<sup>21</sup> Teply et al.<sup>22</sup> observed that radiofrequency ablation combined with injections of 5-FU augmented the efficacy of reducing keloid volume, which is consistent with our findings. Innovatively, our study afforded greater flexibility in selecting the optimal parameters of electrocoagulation based on the thickness of the keloid tissue, thereby achieving higher safety and more favorable outcomes. Needle-assisted electrocoagulation permitted direct drug injection after energy delivery, preventing drug overflow through micropores and enhancing drug absorption.

This study validated the efficacy of needle-assisted electrocoagulation combined with an injection of a corticosteroid and 5-FU

for keloid removal. However, it has several limitations. First, the molecular mechanisms underlying the therapeutic efficacy of ablation combined with pharmacotherapy in treating keloids were not explored. Second, the small sample size and short follow-up period obscured the observation of the long-term prognosis and recurrence rate of keloids. Third, whether other types of thermal ablation and drugs can be applied to patients with keloids requires thorough analysis.

## 5 | CONCLUSION

Ablation combined with pharmacotherapy significantly reduces the volume of keloids by inhibiting angiogenesis, proliferation, and deposition of the extracellular matrix and promoting collagen degradation with high efficacy and safety.

## AUTHOR CONTRIBUTIONS

Jingting Zhao, Xiaoyu Zhai, Zhiyi Xu, Bingrong Zhou and Hui Hua were responsible for designing the experiments; Jingting Zhao, Xiaoyu Zhai and Zhiyi Xu were responsible for performing experiments and data analysis; Shu Zhou and Liqun Gu provided reagents, materials and instruments; Lin Chen was responsible for investigation; Bingrong Zhou and Hui Hua proposed the methodology; Jingting Zhao, Xiaoyu Zhai, Zhiyi Xu contributed to manuscript drafting; Bingrong Zhou and Hui Hua reviewed the manuscript. All authors have approved the submission of this manuscript.

## FUNDING INFORMATION

This work was supported by the Nantong Science Foundation (MS22022102), and the Nantong Young Medical Key Talent Program.

## CONFLICT OF INTEREST STATEMENT

The authors declare no conflict of interest in the publication of this article.

## DATA AVAILABILITY STATEMENT

The data that support the findings of this study are available from the corresponding author upon reasonable request.

## ETHICS STATEMENTS

The study was conducted in accordance with the Declaration of Helsinki and was approved by the Ethics Committee of Nantong Third People's Hospital (No: EL2022016). The study strictly adhered to the protocols sanctioned by the Animal Center at the Medical College of Nantong University (No: S20230426-009).

The patients in this manuscript provided written informed consent for the publication of their case details and clinical pictures.

## REFERENCES

- Lu W, Chu H, Zheng X. Effects on quality of life and psychosocial wellbeing in Chinese patients with keloids. *American Journal of Translational Research*. 2021;13(3):1636-1642.
- Oliveira GV, Metsavaht LD, Kadunc BV, et al. Treatment of keloids and hypertrophic scars. Position statement of the Brazilian expert group GREMCIQ. *Journal of the European Academy of Dermatology and Venereology*. 2021;35(11):2128-2142.
- Ogawa R. Keloid and hypertrophic scars are the result of chronic inflammation in the reticular dermis. *International Journal of Molecular Sciences*. 2017;18(3):606.
- Ogawa R, Dohi T, Tosa M, Aoki M, Akaishi S. The latest strategy for keloid and hypertrophic scar prevention and treatment: the Nippon medical school (NMS) Protocol. *Journal of Nippon Medical School*. 2021;88(1):2-9.
- Hietanen KE, Järvinen TA, Huhtala H, Tolonen TT, Kuokkanen HO, Kaartinen IS. Treatment of keloid scars with intralesional triamcinolone and 5-fluorouracil injections—a randomized controlled trial. *Journal of Plastic, Reconstructive & Aesthetic Surgery*. 2019;72(1):4-11.
- Khalid FA, Mehrose MY, Saleem M, et al. Comparison of efficacy and safety of intralesional triamcinolone and combination of triamcinolone with 5-fluorouracil in the treatment of keloids and hypertrophic scars: randomised control trial. *Burns*. 2019;45(1):69-75.
- Tawaranurak N, Pliensiri P, Tawaranurak K. Combination of fractional carbon dioxide laser and topical triamcinolone vs. intralesional triamcinolone for keloid treatment: a randomised clinical trial. *International Wound Journal*. 2022;19(7):1729-1735.
- Habibi M, Berger RD, Calkins H. Radiofrequency ablation: technological trends, challenges, and opportunities. *Europace*. 2021;23(4):511-519.
- Pinder LF, Parham GP, Basu P, et al. Thermal ablation versus cryotherapy or loop excision to treat women positive for cervical precancer on visual inspection with acetic acid test: pilot phase of a randomised controlled trial. *The Lancet Oncology*. 2020;21(1):175-184.
- Lucas SM, Stern JM, Adibi M, Zeltser IS, Cadeddu JA, Raj GV. Renal function outcomes in patients treated for renal masses smaller than 4 cm by ablative and extirpative techniques. *The Journal of Urology*. 2008;179(1):75-79; discussion 79–80.
- Wu C, Yang JF, Zhang Q, Liu W, Liao K, Hu B. Successful cholangioscopic electrocoagulation for biliary papillomatosis: report covering six cases (with video). *Gastroenterología y Hepatología*. 2021;44(8):546-551.
- Klifto KM, Asif M, Hultman CS. Laser management of hypertrophic burn scars: a comprehensive review. *Burns Dent Traumatol*. 2020;8:tkz002.
- Na J, Zheng Z, Dannaker C, Lee SE, Kang JS, Cho SB. Electromagnetic initiation and propagation of bipolar radiofrequency tissue reactions via invasive non-insulated microneedle electrodes. *Scientific Reports*. 2015;5:16735.
- Taheri A, Mansoori P, Sandoval LF, Feldman SR, Williford PM, Pearce D. Entrance and propagation pattern of high-frequency electrical currents in biological tissues as applied to fractional skin rejuvenation using penetrating electrodes. *Skin Research and Technology*. 2014;20(3):270-273.
- Hantash BM, Renton B, Berkowitz RL, Stridde BC, Newman J. Pilot clinical study of a novel minimally invasive bipolar microneedle radiofrequency device. *Lasers in Surgery and Medicine*. 2009;41(2):87-95.
- Craig VJ, Zhang L, Hagood JS, Owen CA. Matrix Metalloproteinases as therapeutic targets for idiopathic pulmonary fibrosis. *American Journal of Respiratory Cell and Molecular Biology*. 2015;53(5):585-600.
- Clapp C, Ortiz G, Garcia-Rodrigo JF, et al. Dual roles of prolactin and Vaso-inhibin in inflammatory arthritis. *Front Endocrinol (Lausanne)*. 2022;13:905756.
- Hernandez-Bule ML, Toledano-Macias E, Perez-Gonzalez LA, Martinez-Pascual MA, Fernandez-Guarino M. Anti-fibrotic effects of RF electric currents. *International Journal of Molecular Sciences*. 2023;24(13):10986.
- Nicoletti G, Perugini P, Bellino S, et al. Scar remodeling with the Association of Monopolar Capacitive Radiofrequency, electric stimulation, and negative pressure. *Photomedicine and Laser Surgery*. 2017;35(5):246-258.
- Hantash BM, Bedi VP, Kapadia B, et al. In vivo histological evaluation of a novel ablative fractional resurfacing device. *Lasers in Surgery and Medicine*. 2007;39(2):96-107.
- Sripachya-Anunt S, Fitzpatrick RE, Goldman MP, Smith SR. Infections complicating pulsed carbon dioxide laser resurfacing for photoaged facial skin. *Dermatologic Surgery*. 1997;23(7):527-536.
- Teplyi V, Grebchenko K. The usage of radiofrequency ablation for treatment of keloids and hypertrophic scars. *Probl Radiac Med Radiobiol*. 2019;24:561-573.

## SUPPORTING INFORMATION

Additional supporting information can be found online in the Supporting Information section at the end of this article.

**How to cite this article:** Zhao J, Zhai X, Xu Z, et al. Novel needle-type electrocoagulation and combination pharmacotherapy: Basic and clinical studies on efficacy and safety in treating keloids. *J Cosmet Dermatol*. 2024;00:1-12. doi:[10.1111/jocd.16453](https://doi.org/10.1111/jocd.16453)